Research Article | Vol. 30, No. 22 / 24 Oct 2022 / Optics Express 40196
Optics EXPRESS

Possibility of compromising the security of free space optics communications caused by scattering on fog particles

PETER BARCIK* AND OTAKAR WILFERT

Brno University of Technology, Faculty of Electrical Engineering and Communication, Department of Radio Electronics, Technicka 12, 616 00 Brno, Czech Republic
*barcik@vut.cz

Abstract: The paper presents experimental verification of coexistence and entry into a free space optical link channel. A numerical model, which describes the properties of the LOS (Line of Sight) channel and NLOS (Non-Line of Sight) channel, was formulated and experimentally verified. Experimental work includes an outdoor fog experiment which confirms theoretical predictions. It has been shown that under certain optimal conditions (sufficient transmitting power, dense fog, optimal eavesdropper's receiver distance and optimal angle between the eavesdropper's receiver and the axis of the wireless optical link) unauthorized reception is possible.

1. Introduction

The constant development of new standards for wireless communications places increasing demands on individual communication components in terms of transmission speed, transmission capacity, versatility, scalability and energy efficiency. Meeting these requirements requires advanced hardware and technology operating in the new spectrum bands [1]. Optical wireless communications, thanks to their specific features and constant development, occupy a place in modern communication technologies, whether for short or long distances. The planned implementation of optical wireless links in the B5G and 6G standards for mobile communications has been the impulse for denser deployment in cities and built-up areas. Deployment for temporary (ad-hoc) networks between the UAV (Unnamed Aerial Vehicle) and the ground station is also envisaged.

New applications for wireless optical links present problems and challenges that have not yet been addressed, but which can in principle have a major impact on system parameters and security. The properties of an optical wireless connection are highly dependent on the current state of an unstable atmospheric transmission channel. Due to the scattering of the optical wave on aerosols (water droplets, dust) in the atmosphere, there is a possibility of unauthorized detection of the optical signal. For this reason, it can be assumed that there may be attempts to intercept or disrupt the communication. According to [2], information security in FSO (Free Space Optics) communication can be divided into transmission security and communication security. Transmission security focuses mainly on the security of transmission on the physical layer. Communication security is mainly focused on the integrity of messages transmitted by the communication system.

In this article, we will focus mainly on transmission security. We will investigate the possibility of listening to FSO communication by scattering the optical wave on hydrometeors and dust particles in the atmosphere. The article will present a numerical model that defines the basic parameters of the FSO connection and then will present a hypothetical numerical model of the NLOS (Non-Line of Sight) connection (unauthorized). An article that presents a similar model is [3]. However, our article will also present the verification of the numerical model by

#470757 https://doi.org/10.1364/OE.470757
Journal © 2022 Received 19 Jul 2022; revised 27 Sep 2022; accepted 28 Sep 2022; published 14 Oct 2022

Optics EXPRESS

experimental measurements. To the best of our knowledge, a similar experimental measurement has not yet been published.

The structure of the article is organized as follows. Chapter II presents background of atmospheric phenomena and scattering. Chapter III deals with steady state models of authorized and unauthorized connections. Chapter IV presents a comparison of experimental data with theoretical predictions. A discussion about the possibility of eavesdropping on the FSO connection is discussed in Chapter V.

1.1. Related works

Information security, in optical communications generally, became important in the context of increasing coverage and implementation for critical applications (financial, military). The physical layer security in FSO and Visible Light Communication (VLC) links is investigated in [4]. Due to divergence of the laser beam transmitter and turbulence-induced fading on the received irradiance, the FSO link may be tapped by an eavesdropper receiver placed closed to the legitimate receiver [2]. Framework for analysis of the secrecy performance of the secrecy outage probability of an FSO system affected by gamma-gamma turbulence-induced fading channels with pointing errors is presented in [5]. Atmospheric phenomena that significantly affect the function of FSO include the absorption and scattering of light on gas molecules, hydrometeors and lithometeors. Due to light scattering there is the possibility of tapping the FSO link by placing an eavesdropper receiver outside the laser beam [3]. This security issue is a bigger concern in Underwater Optical Communication (UWOC) links where the scattering phenomenon is even stronger. In [6], the numerical investigation of security weakness of UWOC links via the Monte-Carlo simulation is presented. Because of more effective scattering in the UV region, this principle is advantageously (positively) used in Ultra Violet Non Light of Sight (UV-NLOS) communication links where scattered ultraviolet light is received by a legitimate receiver. In [7] the security of NLOS communication systems is investigated.

A number of techniques have been studied which enhance physical layer security in FSO systems. A secure optical communication system with symbol overlapped, optical phase encrypted differential-phase-shift-keying modulated signal is experimentally demonstrated in the paper [8]. A hybrid optical frequency hopping system based on Orbital angular momentum (OAM) multiplexing is proposed in [9]. A secure FSO communication system based on Data Fragmentation Multi-path Transmission (DFMT) scheme is proposed and demonstrated in [10]. Physical layer security challenges in mixed RF/FSO systems are also a concern. Researchers are focused on a dual hop RF/FSO communication system in presence of multiple eavesdroppers [11].

Communication security or message integrity in FSO systems can be provided by the Quantum Key Distribution (QKD) technique. Revision of the Discrete Variable QKD (DV-QKD) and Continuous Variable QKD (CW-QKD) protocols over FSO is discussed in [12]. Quantum technology employed in optical wireless communication in the data-center is presented in [13]. A successful experiment of free space QKD over 53 km carried out in daylight has been demonstrated in [14]. In [15], performance analysis of satellite to ground FSO QKD systems using key retransmission is presented.

2. Atmospherical phenomena

The atmospheric phenomena causes attenuation, fluctuations in the received optical power and shape distortion of the transmitted pulses. In general, attenuation of optical power, fluctuations in optical intensity, and beam interruption are caused by many phenomena. This article summarizes the influence of hydrometeors and lithometeors. Aerosols (hydrometeors and lithometeors) are, from the physiochemical dispersion system of microscopic and submicroscopic points of view, particles generally larger than 0.001 μm and smaller than 100 μm solid or liquid phases

Optics EXPRESS

in a gaseous medium. They can be classified according to dispersity, mechanism of formation (condensation or dispersion aerosol) and phase state. One of the basic characteristics of an aerosol, which other properties depend more or less on, is the size of the part (diameter d). The aerodispersion system containing parts of different sizes is described by statistical distribution functions, or its statistical moments (mean value, mean square value, or others). Due to the wide range of particle sizes, a log-normal distribution is usually used, which is defined by functions [16]

$$f(d) = \frac{1}{d\ \ln(\sigma_g)\sqrt{2\pi}} \exp - \frac{\left(\ln(d) - \ln(d_g)\right)^2}{2\left(\ln(\sigma_g)\right)^2}, \tag{1}$$

where d_g is the geometric mean and σ_g is the geometric standard deviation.

In addition to particle size, there are other parameters that affect the interaction of the aerosol with the optical wave such as complex permittivity, respectively complex refractive index.

Because the changes in optical intensity caused by absorption or scattering are slow with an onset time of a few minutes, the link attenuation will be considered constant in this article. During absorption, photons are absorbed by gas molecules and it is a highly spectrally dependent phenomenon. The scattering distinguishes whether it is the interaction of photons with particles smaller than the wavelength λ of the radiation (Rayleigh scattering) or whether the interaction of photons with particles whose size is comparable to the wavelength of the radiation (Mie scattering). Rayleigh scattering is strongly spectrally dependent, and in the case of Mie scattering it is a spectrally independent phenomenon. If the interaction concerns particles much larger than the wavelength of radiation (water droplets in the rain, etc.), such a phenomenon can be described by a model of geometric optics.

The common consequences of absorption and scattering on the attenuation of optical intensity can be characterized as the so-called extinction phenomenon (attanuation) for which Beer's law applies [17]. The spectral transmittance of a given atmosphere $T_\lambda(\lambda)$ is defined by the relation

$$T_\lambda(\lambda) = \frac{I_2(\lambda)}{I_1(\lambda)}, \tag{2}$$

where the optical intensity at the end of the layer is $I_2(\lambda)$ and the optical intensity at the beginning of the layer of thickness L is $I_1(\lambda)$. For the transmittance the relation holds (Beer's law)

$$T_\lambda = \exp(-\alpha_e(\lambda)L), \tag{3}$$

where $\alpha_e(\lambda)$ is the extinction coefficient in $[m^{-1}]$.

For the energy balance of the FSO link, the quantity meteorological visibility has a practical use, which is defined as the length of the path in the atmosphere L, at which the transmittance takes the value $T = 0.02 = 2\%$ (at $\lambda = 550$ nm). There is an empirical relationship between the meteorological visibility V_M and the extinction coefficient α_e in the VIS and NIR spectrum [18]

$$\alpha_e \approx \frac{3.91}{V_M \left(\frac{550}{\lambda}\right)^q}, \ [km^{-1}; km; nm], \tag{4}$$

where q is empirical constant determined by the size and distribution of the scattering particles and it is equal to $q = 0.16V_M + 0.34$ for 1 km $<V_M<$6 km (haze), $q = V_M - 0.5$ for 0.5 km $<V_M<$1km (medium fog), $q = 0$ for $V_M<$0.5 km (strong fog). The meteorological visibility V_M must be in km units and wavelength in nm units in this model.

Attenuation of optical intensity in the atmosphere can also be characterized by the attenuation coefficient $\alpha_{1,part}$ in $[dB/km]$

$$\alpha_{1,part} = 4.3\,\alpha_e, \ [dB/km; km^{-1}]. \tag{5}$$

Optics EXPRESS

2.1. Scattering

If the transmission medium contains a relatively large concentration of aerosols, the linear size of which is comparable to the wavelength of the interacting radiation, the radiation is predominantly scattered on the aerosols. Given the nature and relative size of the aerosol particles (fog, smoke) that come into consideration in our case, we will assume that the nature of the scattering satisfies elastic Mie scattering. (Scattered photons only change the direction of motion, not the frequency.)

The effective scattering cross section σ_s $[m^2]$ is determined by the particle radius a, the wavelength λ and the refractive index of the particle n and defines the area of the incident plane wave which results in light scattering. The parameter σ_s has an area dimension and is calculated from Mie's scattering theory. By normalizing the effective cross section of the particle σ_s the cross section of the particle itself, we obtain the scattering efficiency related to one particle Q_s [19]

$$Q_s = \frac{\sigma_s}{\pi\, a^2}\ [-]. \tag{6}$$

Because part of the incident light can be absorbed, there is an area of the incident wave that is related to the absorption and is defined by the effective absorption cross section σ_{abs}. The effective extinction cross section σ_{ext} is given by the sum of the two effective cross sections

$$\sigma_{ext} = \sigma_s + \sigma_{abs}. \tag{7}$$

The extinction efficiency parameter is defined similarly to the scattering efficiency parameter

$$Q_{ext} = \frac{\sigma_{ext}}{\pi\, a^2}\ [-]. \tag{8}$$

In this paper, we quantify the magnitude of the scattering using the volume scattering coefficient β_r. For the theoretical determination of the numerical value of the volume scattering coefficient, we used the analysis given in [20], where it is stated that the numerical value of the volume scattering coefficient per one particle with effective cross section σ_s irradiated by unit optical intensity ($1\ W.m^{-2}$) with length wave λ_L corresponds to the elementary optical power $dP_r(\Theta_V)$ scattered by the unit scattering volume in region C to the elementary solid angle $d\Omega_r$ in the direction Θ_V, see Fig. 1. Expressed mathematically:

$$\beta_r(N, a, C, \Theta_V) = N(C)\,\sigma_s\,\frac{1}{4\pi}\,p(\Theta_V) = N(C)\,\frac{\pi a^2}{4\pi}\,Q_s\,p(\Theta_V),\ [m^{-1}sr^{-1}], \tag{9}$$

where $N(C)$ is number of scattering particles in the region C, a is the mean radius of the particle, Q_s is scattering efficiency of the one particle and $p(\Theta_V)$ is the phase scattering function in the direction Θ_V. The total volume scattering coefficient b_r, which is not dependent on the angle Θ_V, is given as follows

$$b_r(N, a, C) = N(C)\,\sigma_s = N(C)\,\pi\,a^2\,Q_s,\ [m^{-1}]. \tag{10}$$

By normalizing the volume scattering coefficient β_r with respect to the total volume coefficient of variance b_r we get the phase function of variance

$$p(\Theta_V) = \frac{\beta_r(N, a, C, \Theta_V)}{b_r(N, a, C)},\ [sr^{-1}]. \tag{11}$$

The scattering phase function $p(\Theta_V)$ provides information on the relative angular distribution of the volume scattering coefficient.

Knowing the optical power of the laser transmitter P_{TX}, the phase scattering function can be used for the theoretical calculation of the detected scattered optical power $P_r(\Theta_V)$ in the direction

Optics EXPRESS

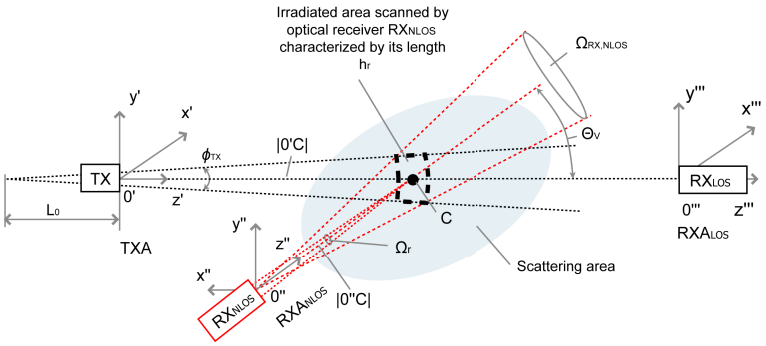

Fig. 1. Illustration of the LOS and NLOS FSO system architecture. TX - laser transmitter; ϕ_{TX} - is the area angle corresponding to the divergence of the radiated beam; 0'x'y'z' - coordinate system for the transmitter; RX_{NLOS} - NLOS optical receiver; 0"x"y"z" - coordinate system for the NLOS receiver; RX_{LOS} - LOS optical receiver; 0"'x"'y"'z"' - coordinate system for the LOS receiver; C - center of the scanned area; |0'C| - the distance between the laser transmitter and point C; |C0"| - the distance between point C and the NLOS optical receiver; |0'0"'| - distance between transmitter and LOS optical receiver; L_0 - length for propagation attenuation calculation; Ω_r - solid angle in which the scattered radiation propagates to the optical receiver; $\Omega_{RX,NLOS}$ - solid angle of the NLOS optical receiver; Θ_V - scanning angle of the irradiated area of the scattering medium.

Θ_V as follows

$$P_r(\Theta_V) = N(C)\,\frac{\pi a^2}{4\pi}\,Q_s p(\Theta_V)\,P_{TX}\,\Omega_r\,h_r\,\exp\left(-N(C)\sigma_{ext}|0'0''|\right),\ [W] \tag{12}$$

where $|0'0''|$ is the length of the route from the transmitter to the receiver and h_r is the length of the scanned area (given by the receiver angle of view Ω_r and the scanning angle Θ_V).

3. Steady system model

The subject of our article is to create a system model and experimentally verify the possibility of illegitimate entry into the FSO connection channel by means of scattering on hydrometeors. In this paper, we approach the connection between the transmitter and the legitimate receiver as a free space optical link with direct line-of-sight (LOS FSO). We treat the connection between the transmitter and the eavesdropper's receiver as a free space optical link with indirect visibility between terminals (NLOS FSO; Non-Line of Sight Links). NLOS FSO is assumed to operate according to Mie's principle of light scattering on aerosols (see Fig. 1). In literature dealing with the security of transmitted information, the transmitter terminal (TX) is usually referred to as Alice, legitimate receiver (RX_{LOS}) as Bob and eavesdropper's receiver (RX_{NLOS}) as Eve.

3.1. Line of Sight FSO steady model

We model the connection between the transmitter and the legitimate receiver (RX_{LOS}) using a steady system model as follows. Let the total attenuation of the FSO link be denoted by

$$\alpha_{tot} = \alpha_{TX} + \alpha_{12} + \alpha_{atm} + \alpha_{RX,LOS}, \tag{13}$$

where α_{TX} is attenuation on all of the transmitter's (TX) optical elements, $\alpha_{RX,LOS}$ is the attenuation on all of the receiver's (RX_{LOS}) optical elements and α_{atm} is atmospheric attenuation.

Optics EXPRESS

The propagation attenuation is stated as follows

$$\alpha_{12} = \left| 20 \log \frac{L_0}{L_0 + L_{12}} \right|, \tag{14}$$

where L_0 is auxiliary length for propagation attenuation calculation and $L_{12} = |0'0'''|$ is distance between transmitter aperture (TXA) and receiver aperture (RXA_{LOS}). To express L_0, it is necessary to know the diameter of the transmitter's aperture D_{TXA} and the divergence of the transmitting beam ϕ_{TX}. The expression for the auxiliary length L_0 applies

$$L_0 \approx \frac{D_{TXA}}{\phi_{TX}}. \tag{15}$$

Propagation attenuation α_{12} and gain on the receiving aperture $\gamma_{RXA,LOS}$ are usually included in a single quantity called geometric attenuation α_{geom}

$$\alpha_{geom} = \left| 20 \log \frac{D_{RXA,LOS}}{D_{TXA} + \phi_{TX} L_{12}} \right| \approx \left| 20 \log \frac{D_{RXA,LOS}}{\phi_{TX} L_{12}} \right| \ [dB]. \tag{16}$$

The received power in dB by RX_{LOS} is given as follows:

$$P_{RX,LOS}(L_{12}) = P_{TX} - \alpha_{TX} - \alpha_{geom}(L_{12}) + \gamma_{add} - \alpha_{RX,LOS} - \alpha_{atm}(L_{12}) \ [dBm], \tag{17}$$

where γ_{add} is additional gain due to gaussian beam distribution. Assume that atmospheric attenuation is predominantly caused by scattering on aerosol particles $\alpha_{atm} = \alpha_{aer} = \alpha_e L_{12}$ $[dB]$ and the dependence of the attenuation of the atmosphere on the distance L_{12} is linear (it works in the near region).

An important variable for evaluating the energy balance of the FSO link is the link margin M_{LOS} defined as

$$M_{LOS}(L_{12}) = P_{RX,LOS}(L_{12}) - P_{MIN,LOS} - SNR_{RX,LOS} \ [dB], \tag{18}$$

where $P_{MIN,LOS}$ is the minimal detectable power of the optical receiver and $SNR_{RX,LOS}$ is the required signal-to-noise ratio in the optical domain.

3.2. Non-line of sight FSO steady model

Illegitimate reception using an eavesdropper receiver (RX_{NLOS}) can be modeled using the Eq. (12). This equation can be reformulated to express the total attenuation α_r of an optical wave propagating from a laser transmitter to an eavesdropper receiver:

$$\alpha_r = \frac{P_{RX,NLOS}}{P_{TX}} = \beta_r(N, a, C, \Theta_V)\, \Omega_{RX,NLOS}\, h_r \, \exp\left(-N(C)\sigma_{ext}|0'0''|\right) \xi_{RX,NLOS}, \ [-] \tag{19}$$

where the solid angle of the NLOS receiver is $\Omega_{RX,NLOS} = \frac{\pi D^2_{RX,NLOS}}{4|C0''|^2}$, length of the scanned area is $h_r = 2|C0''| \tan \frac{d_{PD}}{2f_{RX,NLOS}} \frac{1}{1+\cos\Theta_V}$ and $\xi_{RX,NLOS}$ is system efficiency of the NLOS receiver.

The power balance equation in decibel scale was derived for the stationary energy balance of the NLOS FSO link

$$\begin{aligned} P_{RX,NLOS}(N, a, C, \Theta_V) = P_{TX} - K_s(P_{RX,NLOS}, \Omega_{RX,NLOS}) - K_{aer}(N, A, C, \Theta_V) \\ + G_{RXA} + G_{PD} - 10 \log |C0''|, \ [dBm] \end{aligned} \tag{20}$$

where K_s is the system function which characterizes the eavesdropper receiver RX_{NLOS}, K_{aer} is the function which characterizes scattering parameters, G_{RXA} is the gain given by the receiving

Optics EXPRESS

lens, G_{PD} is the gain of the photodiode. The functions are defined as follows

$$K_s = 10 \log \left(\frac{\pi}{4} \frac{d_{PD} D_{RX,NLOS}^2}{f_{RX,NLOS}} \xi_{RX,NLOS} \right), \tag{21}$$

$$K_{aer} = 10 \log \left(\beta_r(N, a, C, \Theta_V) \exp \left(-\sigma_{ext} |0'0''| \right) \right), \tag{22}$$

where d_{PD} is the diameter of the receiver's photodiode, $D_{RX,NLOS}$ is the diameter of the receiving lens, $f_{RX,NLOS}$ is the focal length of the receiving lens and $\xi_{RX,NLOS}$ is the efficiency of the receiving optical system.

The margin of the NLOS FSO link (M_{NLOS}) depends on the characteristics of the scattering environment and on the system parameters of the link (see Fig. 1)

$$M_{NLOS} = P_{RX,NLOS} - P_{MIN,NLOS} - SNR_{RX,NLOS} \tag{23}$$

where $P_{RX,NLOS}$ is the scattered optical power received by RX_{NLOS}; $P_{MIN,NLOS}$ is the minimal detectable power of the RX_{NLOS} receiver and SNR_{NLOS} is the required signal-to-noise ratio in the optical domain.

3.3. Synthesis

The synthesis of LOS and NLOS FSO links consists of drawing a graph, where on the vertical axis there will be M_{LOS} and M_{NLOS} and on the horizontal axis there will be the extinction coefficient α_e; the parameters will be the distances of the LOS and NLOS link. Transmitter power and receiver sensitivity are among the system parameters of the links. The parameters of the simulation are specified in figure caption. Finding the M_{NLOS} value using the graph in Fig. 2 shall proceed as follows. According to the parameters given by the elements of the LOS FSO link, the reserve of the M_{LOS} connection is calculated (12.3 dB is indicated in Fig. 2). For the relevant L_{LOS} distance (e.g. 500 m) we determine the magnitude of the extinction coefficient of the atmosphere, which is around 0.015 1/m. The extinction coefficient was estimated according to experimental measurement published in the scientific paper [21]. Subsequently, according to the parameters

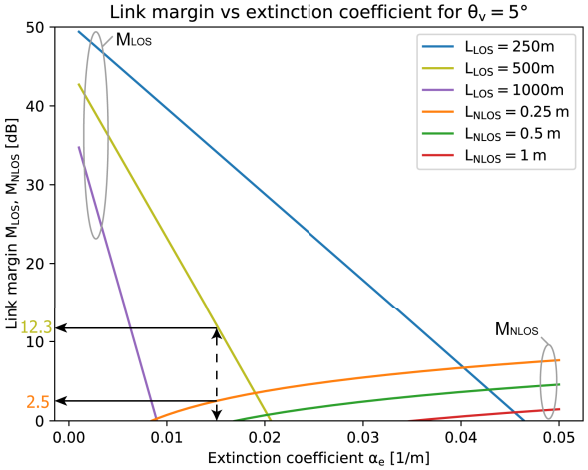

Fig. 2. Link Margin for LOS and NLOS systems depending on the attenuation coefficient for scanning angle Θ_v = 5° and wavelength λ = 1550 nm. (P_{TX} = 20 dBm, $P_{MIN,LOS}$ = -43 dBm, $SNR_{RX,LOS}$ = 3 dB, $P_{background}$ = -70 dBm, $D_{RX,LOS}$ = 120 mm, Θ_{TX} = 1 mrad; α_{TX} = 3 dB, α_{RX} = 4 dB, γ_{add} = 3.7 dB, $P_{MIN,NLOS}$ = -68.9 dBm, SNR_{NLOS} = 3 dB, $D_{RX,NLOS}$ = 120 mm, $f_{RX,NLOS}$ = 120 mm, d_{PD} = 0,15 mm, $\xi_{RX,NLOS}$ = 1, $SNR_{RX,NLOS}$ = 3 dB)

Optics EXPRESS

given by the NLOS FSO link elements, we find the numerical value of the NLOS FSO margin M_{NLOS} (from the figure it is 2.5 dB), and thus we get the qualitative parameter which assesses the possibility of compromising the LOS FSO communication.

4. Experimental measurement

The workplace on the roof of the Brno University of Technology building was used to verify the above mentioned theoretical models and the possibility of eavesdropping on the FSO connection. The fog maker Look Unique 2.1 was used as the fog generator. The fog parameters (particle concentration and particle size distribution) were measured with the Sensirion SPS30 optical sensor. The parameters of the LOS and NLOS receiver are summarized in Table 1.

The arrangement of the experiment was according to Fig. 3. An SFP module was used as the signal source, which generated a pulse with a length of 10 ns with a frequency of 10 Hz using an FPGA kit. The optical pulse with a wavelength of 1550 nm was amplified by an EDFA amplifier. The single-mode fiber connected to the EDFA output, irradiated a transmitting lens with a diameter of D_{TX} = 25.4 mm and a focal length of f_{TX} = 35 mm. The divergence of the transmitting optical wave was set similarly to the real FSO transmitter, i.e. ϕ_{TX} = 1 mrad (edge-to-edge). As the RX_{LOS} receiver, an optical power detector (Avantes) with receiver lens diameter $D_{RX,LOS}$ = 50.8 mm and a focal length $f_{RX,NLOS}$ = 50 mm was used. The measurement procedure was as follows. Firstly, the fog generator was activated. Then continuous recording of the data from the LOS receiver, NLOS receiver and particle sensor started. From the received optical power by the RX_{LOS} receiver, the extinction coefficient was calculated. Measured power from the RX_{LOS} receiver as a function of extinction coefficient is presented in Fig. 4. The fog generator was located around 1 m from the transmitter. For better temporal and spatial stability of the generated fog, a plexiglass wind shield was used around the intersection area. The scattered radiation from fog particles was detected by an optical receiver RX_{NLOS} at a distance |C0”| = 0.5 m from the point of intersection of the laser beam and the fog area (C). The scattering angle Θ_V was varied so that the angular scattering dependence could be measured sequentially for angles of 10 °, 17°, 30°, 40°, 50°, 90° and 163°. Scattered laser radiation was focused on an InGaAs photodiode Thorlabs FGA015 with an active surface diameter d_{PD} = 0.15 mm using a lens with a diameter of $D_{RX,NLOS}$ = 50.8 mm and a focal length of $f_{RX,NLOS}$ = 50 mm. Because the signal from the photodiode was weak, it was amplified using an MAX 2650 amplifier (with gain 18 dB) and two RF amplifiers with 30 dB gain each. The signal was then recorded using an oscilloscope.

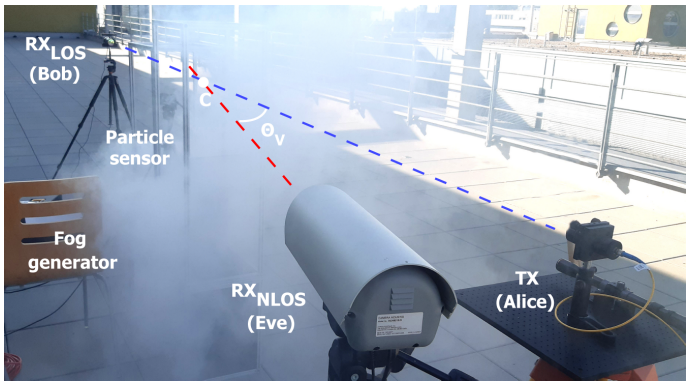

Fig. 3. Experimental workplace on the roof of the faculty building.

Optics EXPRESS

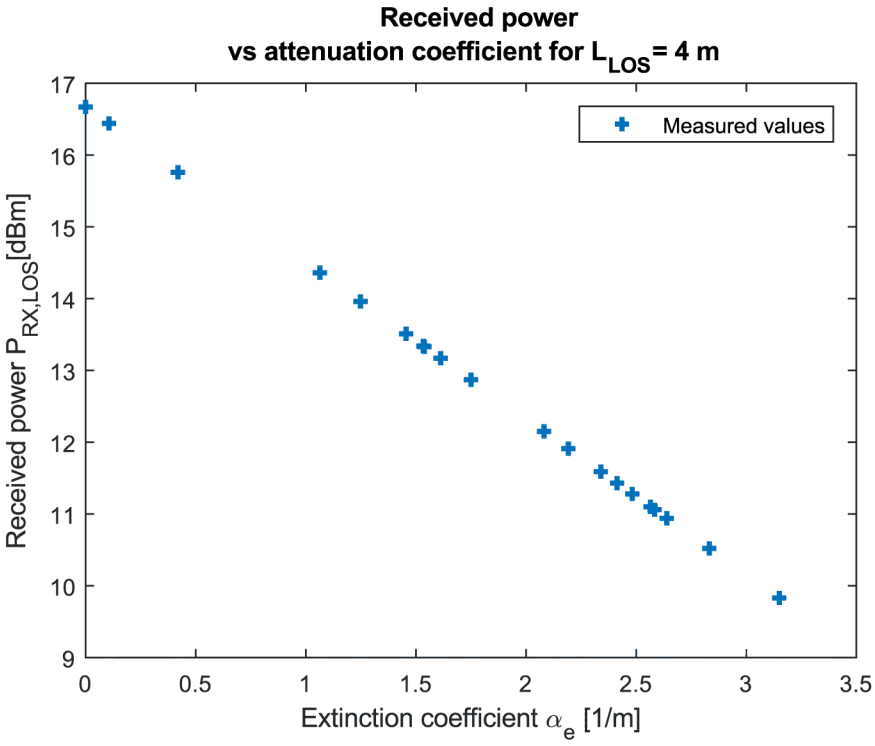

Fig. 4. Measured power received by the LOS receiver vs. extinction parameter.

Table 1. Parameters of the LOS and NLOS receiver

Parameter	RX_{LOS}	RX_{NLOS}
Saturation level SAT [dBm]	-1	-32
Minimal detectable power P_{MIN} [dBm]	-43	-68.9
Dynamic range [dB]	42	36.9
Peak sensitivity [nm]	1450	1550
Receiving lens diameter [mm]	50.8	50.8

Figure 5 presents the measured and theoretical received power by RX_{NLOS} for three different scanning angles θ_V. The theoretical received power by RX_{NLOS} was calculated according to Eq. (19). To calculate the volume scattering function we used Eq. (9). The effective scattering cross section σ_s and phase function $p(\theta_v)$, for specific size of the particle and scanning angle θ_v, were calculated with Mie python package [22]. It was found that measured values of scattered power follow the theoretical trend. To better compare the theoretical model, more data (received scattered power) need to be gathered and averaged. In our opinion, this is the reason why the measured data doesn't fit better with the theoretical model.

In Fig. 6 the measured portion of the scattering phase characteristic is shown. To measure the phase scattering function we made measurements for different angles θ_v. To calculate the volume scattering coefficient β we used the average value of the scattered power from 50 measurements. From the vector of calculated β values, the total volume scattering function b_r was calculated by integration β over all angles (4π sr). The scattering phase function was calculated by normalization of β by total volume scattering function b_r. We assume that the phase characteristic is symmetric with respect to the beam axis. By comparing the measured

Optics EXPRESS

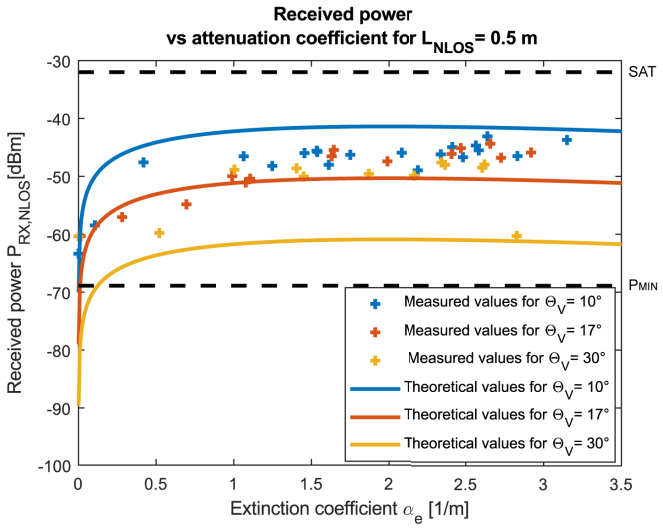

Fig. 5. Measured and theoretically calculated power received by NLOS receiver vs. extinction parameter for different scanning angles θ_V. P_{MIN} - minimal detectable power of the RX_{NLOS} optical receiver , SAT - saturation level of the RX_{NLOS} optical receiver.

phase function with the theoretical one, it is possible to estimate the radius of the scattering particles. In our case, the radius of the scattering particles is about 0.8 μm. From Fig. 6 it is also possible to see that eavesdropping is most effective for angles $\theta_V \approx 0°$. On the other hand, the risk of eavesdropping for angle $\theta_V \approx 90°$ is minimal. Subsequently, we measured the particle size and concentration with particle meter Sensirion SPS30 which was placed near the measured region C. The average radius of the particles measured by Sensirion was 0.8 μm. The measured concentration of the particles smaller than 1 μm was $2.10^5\ \#/cm^3$.

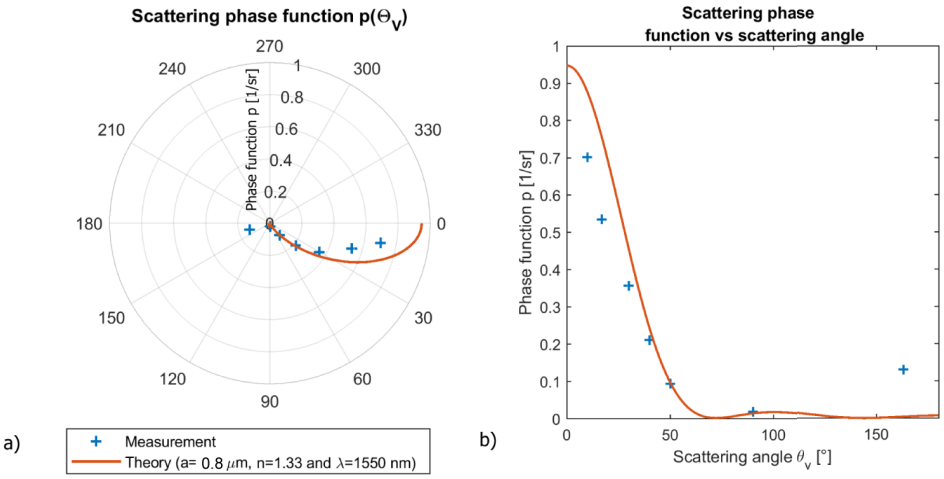

Fig. 6. Measured (a) and theoretically calculated (b) phase scattering function for particle radius a = 0.8 μm, wavelength λ = 1550 nm and refractive index n = 1.33.

The measured scattered optical power together with theoretically calculated values presented in Fig. 6 support the Mie scattering nature of the experiment. It is clear that with increasing the scattering angle the received scattered optical power decreases.

Optics EXPRESS

5. Discussion

The practical measurements of our research were conducted in order to determine the level of optical power received in the conditions of scattering of laser radiation on aerosols (in fog). The scattered area was determined by the intersection of the laser beam and the viewing angle of the optical receiver. The received power of the optical radiation scattered on a given aerosol can be increased by increasing the area of the receiving aperture and the connection of the APD (Avalanche photodiode) with higher sensitivity. Increasing receiver aperture and the sensitivity of the receiving photodiode on the other hand results in an increase in noise level due to background radiation. From the point of view of FSO connection security, the location of the eavesdropping receiver close to the transmitter for $\theta_V \approx 0^\circ$ angles is critical, where eavesdropping is most effective. The optical power of the transmitter is also very important from the physical security point of view. The higher the power of the transmitter, the greater the risk of eavesdropping is. From the theoretical study and experimental measurement it is clear that scattering on fog particles is most effective for $\alpha_e > 1m^{-1}$, which corresponds to extremely dense fog. The effect of this fog on the entire FSO link would cause the link to malfunction. Therefore, in this work we assume that the fog will act locally, not on the entire route of the FSO link. This will meet the condition that the LOS FSO will be functional and at the same time the received optical power scattered on the fog particles will be large enough. The location of the eavesdropper near the transmitter is ideal because the optical power is strongest. From the perspective of the eavesdropper, the ideal position is somewhere in the middle between the transmitter and the receiver, so that the eavesdropper will be not exposed. However, it is very difficult to find the laser beam with a divergence 1 mrad if one doesn't know exactly the position of the transmitter and receiver. At the receiver, the optical power is usually already poor due to propagation losses, and eavesdropping by scattering is less effective. In conclusion, it can be stated that the FSO connection can be intercepted if the above conditions are met. However, in real conditions, when the FSO transceiver is located on a roof or other inaccessible locations, the risk of eavesdropping is minimal.

6. Conclusion

In this paper, we investigated the possibility of disrupting the physical layer security of the free space optics communication link with unauthorized detection of scattered optical power on fog particles. The steady state models for a legitimate and non-legitimate communication link were formulated. To verify the theoretical models, an experimental measurement was carried out. From the experimental data the optimal conditions for non-legitimate detection were stated. Theoretical models supported by experimental data show that there is the possibility of eavesdropping on the FSO link.

Funding. Ministerstvo Vnitra České Republiky (VI20192022173).

Disclosures. The authors declare no conflict of interest.

Data availability. Data underlying the results presented in this paper are not publicly available at this time but may be obtained from the authors upon reasonable request.

References

1. A. Parsinen, M. Alouni, M. Berg, T. Kuerner, P. Kyosti, M. Leinonen, M. Matinmikko-Blue, E. McCune, U. Pfeiffer, and P. Wambacq, "White Paper on RF Enabling 6G – Opportunities and Challenges from Technology to Spectrum," 6G Research Visions **13**, 1–68 (2020).
2. F. J. Lopez-Martinez, G. Gomez, and J. M. Garrido-Balsells, "Physical-layer security in free-space optical communications," IEEE Photonics J. **7**(2), 1–14 (2015).
3. D. Zou and Z. Xu, "Information Security Risks Outside the Laser Beam in Terrestrial Free-Space Optical Communication," IEEE Photonics J. **54**, 101821 (2022).

Optics EXPRESS

4. M. Obeed, A. M. Salhab, M. S. Alouini, and S. A. Zummo, "Survey on Physical Layer Security in Optical Wireless Communication Systems," *Comnet 2018 - 7th International Conference on Communications and Networking* pp. 1–5 (2019).
5. R. Boluda-Ruiz, A. García-Zambrana, B. Castillo-Vázquez, and K. Qaraqe, "Secure communication for FSO links in the presence of eavesdropper with generic location and orientation," Opt. Express **27**(23), 34211–34229 (2019).
6. M. Kong, J. Wang, Y. Chen, T. Ali, R. Sarwar, Y. Qiu, S. Wang, J. Han, and J. Xu, "Security weaknesses of underwater wireless optical communication," Opt. Express **25**(18), 21509–21518 (2017).
7. Y. H. Chung Ambrish, "Secure NLOS ultraviolet communication against active/passive eavesdropping attacks," Opt. Commun. **501**, 127378 (2021).
8. Z. Gao, Y. An, A. Wang, P. Li, Y. Qin, Y. Wang, and X. Wang, "40Gb/s Secure Optical Communication Based on Symbol-by-Symbol Optical Phase Encryption," IEEE Photonics Technol. Lett. **32**(14), 851–854 (2020).
9. Y. Jin, Y. F. Chen, C. D. Xu, Y. C. Qi, S. K. Chen, W. Chen, and N. H. Zhu, "A hybrid optical frequency-hopping scheme based on OAM multiplexing for secure optical communications," in *Asia Communications and Photonics Conference 2020*, (2021), pp. 1–3.
10. Q. Huang, D. Liu, Y. Chen, Y. Wang, J. Tan, W. Chen, J. Liu, and N. Zhu, "Secure free-space optical communication system based on data fragmentation multipath transmission technology," Opt. Express **26**(10), 13536–13542 (2018).
11. D. R. Pattanayak, V. K. Dwivedi, V. Karwal, A. Upadhya, H. Lei, and G. Singh, "Secure Transmission for Energy Efficient Parallel Mixed FSO/RF System in Presence of Independent Eavesdroppers," IEEE Photonics J. **14**(1), 1–14 (2022).
12. P. V. Trinh, A. T. Pham, A. Carrasco-Casado, and M. Toyoshima, "Quantum Key Distribution over FSO: Current Development and Future Perspectives," in *Progress in Electromagnetics Research Symposium*, (2018), pp. 1672–1679.
13. S. Arnon, "Quantum technology for optical wireless communication in data-center security and hacking," *Proc. SPIE 10945, Broadband Access Communication Technologies XIII, 109450H*, (2019), February 2019, pp. 1–5.
14. S. K. Liao, H. L. Yong, and C. Liu, "Long-distance free-space quantum key distribution in daylight towards inter-satellite communication," Nat. Photonics **11**(8), 509–513 (2017).
15. N. D. Nguyen, H. T. T. Pham, V. V. Mai, and N. T. Dang, "Comprehensive performance analysis of satellite-to-ground FSO/QKD systems using key retransmission," Opt. Eng. **59**(12), 1–25 (2020).
16. W. Hinds C., "Aerosol Technology: Properties, Behavior, and Measurement of Airborne Particles," in *Aerosol Technology: Properties, Behavior, and Measurement of Airborne Particles*, (Wiley Interscience, 1999), chap. 4, p. 504, 2nd ed.
17. L. C. Andrews and R. L. Phillips, *Laser Beam Propagation Through Random Media*, Press Monographs (SPIE, 2005).
18. I. I. Kim, B. McArthur, and E. J. Korevaar, "Comparison of laser beam propagation at 785 nm and 1550 nm in fog and haze for optical wireless communications," Proc. SPIE **4214**, 26–37 (2001).
19. A. Ishimaru, "Wave propagation and scattering in random media," in *Wave propagation and scattering in random media*, (IEEE and Oxford University, 1997), chap. 2, pp. 9–18.
20. M. Curtis, E. Boss, and C. Roesler, "Ocean Optics Web Book," https://www.oceanopticsbook.info.
21. M. Grabner and V. Kvicera, "Fog attenuation dependence on atmospheric visibility at two wavelengths for FSO link planning," in *2010 Loughborough Antennas and Propagation Conference, LAPC 2010*, (IEEE, 2010), November, pp. 193–196.
22. S. Prahl, "Miepython module," https://miepython.readthedocs.io.